NANO LETTERS

2005
Vol. 5, No. 3
549−553

Sculpting Nanoelectrodes with a Transmission Electron Beam for Electrical and Geometrical Characterization of Nanoparticles

Henny W. Zandbergen,*,†,‡ Robert J. H. A. van Duuren,† Paul F. A. Alkemade,† Günther Lientschnig,† Oscar Vasquez,† Cees Dekker,† and Frans D. Tichelaar†

Kavli Institute of NanoScience, Delft University of Technology, 2628 CJ Delft, The Netherlands, and Department of Chemistry and Princeton Institute for Systems and Materials, Princeton University, Princeton, New Jersey 08544

Received January 18, 2005

ABSTRACT

A method to produce metal electrodes with a gap of a few nanometers with a highly focused electron beam in a transmission electron microscope (TEM) is described. With this method the electrical and geometrical characterization of the same particle is possible. The *I*–*V* characteristics of a gold particle trapped between such electrodes showed the expected single-electron tunneling behavior, with a Coulomb gap corresponding to the geometry of the particle as observed with high-resolution TEM.

In the field of molecular electronics,[1−4] many challenges exist such as the electrical characterization of *individual* molecules or nanoclusters and their contacting and assembly on a small as well as large scale. A key physical characterization is the determination of the current−voltage curves[5−8] of the molecule or nanocluster. Since a number of complications can occur in the molecular assembly, resulting in spurious electrical measurements, visual inspection after, if not during, the electrical measurements is highly desirable to confirm that indeed one particle of the correct type is trapped between the electrodes.

Given the size of target molecules or nanoclusters, there is a clear need for a reliable technique of making electrodes with a gap of only a few nm. Several methods for making such electrodes for molecular electronics have been developed. High-resolution electron beam lithography has been used for the manufacturing of gaps[9,10] down to 6 nm. This approach has the advantage that conventional semiconductor procedures can be followed and that many devices can be made in the same process step. However, the reproducibility is poor and one needs a separate measurement of the actual gap size. Two electrodes with a narrow gap can be made from a single wire by bending the substrate onto which the wire is attached[5] or by passing a high current through the wire, viz. by electromigration.[11] The fabrication and characterization of such break junctions is rather complex and not very reproducible. Alternatively, one can fabricate electrodes via electrochemical deposition and etching; the gap width is then tuned by monitoring the electrical resistance.[12,13] This technique is fairly easy; it in principle allows nanometric precision and is reproducible. A disadvantage of all these methods, however, is that visual inspection of the trapped particle with a high-resolution transmission electron microscope (HRTEM) after or during the physical measurements cannot be done.

Recently we have shown[14] that one can use a highly focused electron beam in a TEM to reduce the size of holes in thin amorphous SiO_2 membranes with nanometer precision. Others have used an electron beam in a TEM to modify metals or carbon nanotubes,[15] for example, to study the atomic structure of nanometer sized and sub nanometer sized gold wires[16−19] made in a TEM. Although gaps were sometimes formed in the process of these investigations,[20] it was not for the purpose of making electrodes. In this paper we show that it is possible to reshape metals in a TEM, in particular gold and platinum, for the controlled manufacturing of electrodes with nanometer-sized gaps, free-standing or on a supporting membrane. In addition we show that these electrodes can be used to trap particles for electrical characterization and subsequent imaging in the TEM.

For the controlled manufacturing of the nanoelectrodes we used a Philips CM-300 UT-FEG operated TEM at an accelerating voltage of 300 kV. Spot sizes between 2 and

* Corresponding author. E-mail: H.W.Zandbergen@tnw.tudelft.nl.
† Delft University of Technology.
‡ Princeton University.

10.1021/nl050106y CCC: $30.25 © 2005 American Chemical Society
Published on Web 02/04/2005

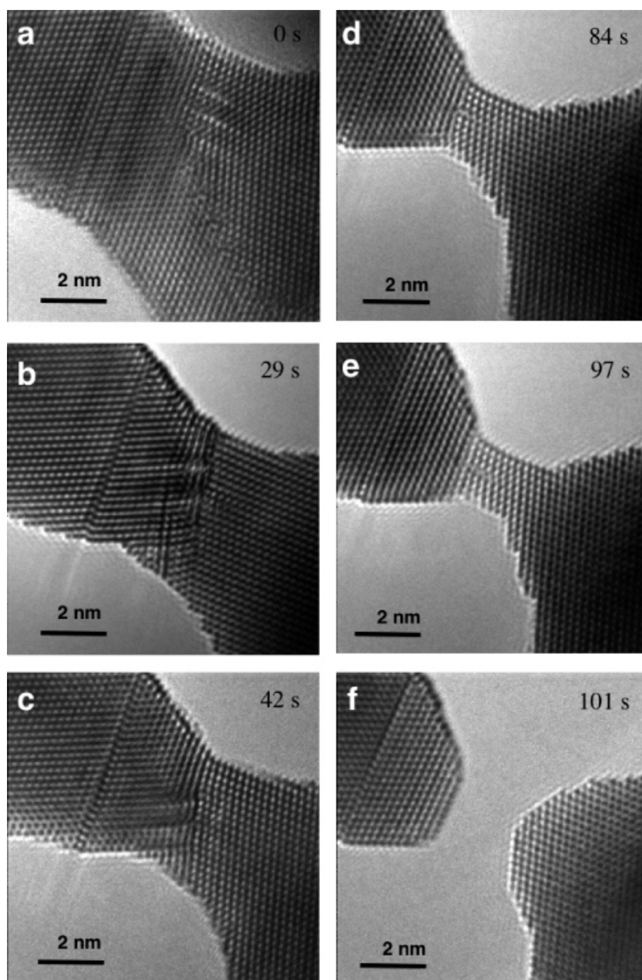

Figure 1. Selection of images from a movie[21] of the formation of a gap, starting with a bridge in a free-standing Au film. The hole in the upper right corner was made by ion beam etching and the one in the lower left by electron beam irradiation prior to the recording of this series. The irradiation times for the recordings are indicated. Upon electron beam irradiation, a 2 nm gap is created (panel f).

10 nm were used with a current of about 5 nA, corresponding to a flux of $\sim 10^9$ electrons/s(nm)^2. Au and Pt lines, 5−10 nm thick and 150 nm wide, were deposited onto a ~1 nm Ti sticking layer on 40 nm thick silicon nitride membranes that were etched as 50 μm by 50 μm large windows in Si. The metal line patterns were defined by electron-beam lithography. The Pt lines were further shaped with a focused ion beam. For the latter we used a 1 pA and 30 keV Ga^+ beam of a FEI Strata 238 Dual-Beam instrument.

Figure 1 shows a series of images taken from a movie[21] of the formation of a pair of electrodes in a 10 nm thick free-standing bicrystalline [110] oriented Au film. First, holes were made with the electron beam to create a 20 nm wide bridge. Next, the bridge was thinned down gradually during continuous monitoring with a fast camera (see Figure 1). When the bridge broke (1E−F), both sides retracted quickly (within 0.1 s; see movie[21]), creating a gap of about 2 nm. This gap could be enlarged by continued electron beam irradiation. After cessation (or major reduction) of the intensity, the electrode ends changed only marginally. From the lattice image contrast before and after the formation of the gap it is concluded that both electrodes in Figure 1F are at the same height. In a number of cases, however, the two electrodes were found not to be at the same height. Thus, the actual gap distance can be larger than is apparent in a TEM image. Likely, release of the nonisotropic, irradiation-induced stresses may cause curling of the electrode ends.

To reduce curling of the electrodes, manufacturing of nanoelectrodes was also done with polycrystalline Au lines deposited on 40 nm thick silicon nitride membrane. The lines used were 10 nm thick and 150 nm wide. During the modification of the Au line, the silicon nitride membrane was also removed. The local disappearance of the membrane has the additional advantage that any nonintentional metal particles in close proximity to the gap are removed as well. Furthermore, the hole in the substrate below and around the gap allows high-resolution TEM inspection of molecules trapped in the gap. Best control over the manufacturing of the electrodes was obtained if the Au line was facing the electron beam. Gaps in the range of 1 to 5 nm were obtained and curling was minimal.

Since the mobility of Pt atoms is much lower than that of Au, we also tested TEM modification of Pt lines. Because of the lower modification speed, we first made a narrow bridge in the lines with a focused ion beam. Figure 2 shows two examples of a series of images of the sculpting of a Pt line on top of a 40 nm thick silicon nitride membrane. Sculpting was indeed feasible but proceeded about 10 times slower than for gold. It took 15 to 60 min of electron irradiation to form electrode pairs from such Pt bridges. The smallest gap size made in Pt was only 0.6 nm. We again note that, due to the removal of the substrate, the electrode pairs were free-standing right at the gap.

Control of irradiation-induced recrystallization and atom transport appears to be important in the full control of the nanoelectrodes. Upon the removal of Pt, and to a lesser extent for Au as well, sometimes single crystalline grains were formed that were elongated in the electron beam direction. One can even push these Pt grains in front of the electron beam by a slow shift of the beam, as if the beam were a snow shovel. Once such grains had been formed, it was very difficult to cut through the grains and thus one had to work around them to create a gap, which often had a reduced stability. We also note that a 6 nm wide electron beam resulted in much more undesired recrystallization than did a 2 nm beam of the same intensity.

After their creation, the gaps widened as a function of time, depending on the metal and the morphology. The strongest widening was observed for polycrystalline gold (up to several nanometers for the first 30 min, despite a strong reduction in applied beam intensity). In particular, this was the case for sharp tips. For single crystalline Au and polycrystalline Pt, the widening was between negligible and 1 nm under similar conditions. The continued change in shape was probably due to stress relaxation and lowering of the surface energy.

The electron-beam-induced changes are related to atom diffusion along surfaces and grain boundaries. Lateral atom

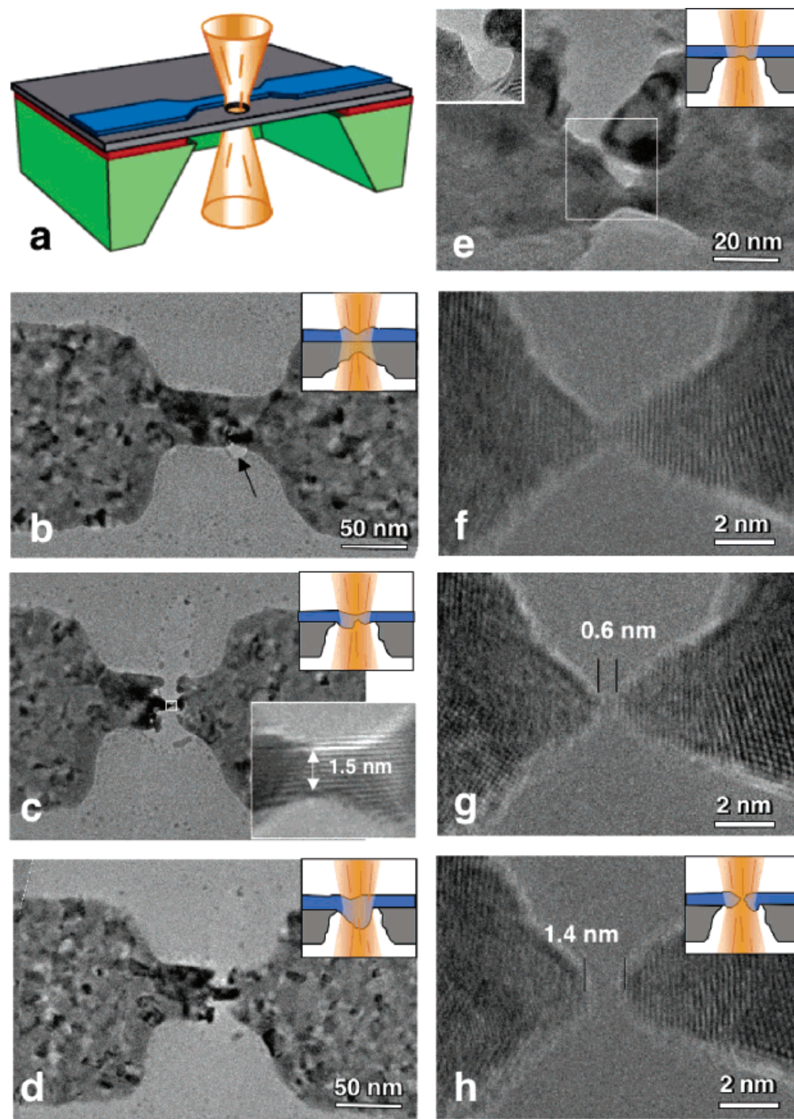

Figure 2. Schematic picture (a) of a device with a polycrystalline metal line (blue) on top of a ~40 nm SiN membrane (grey, on top of SiO_2 (red) and Si (green)) and a selection of TEM images of two runs to fabricate gaps in a 150 nm wide Pt line. Initially 50 nm wide bridges in the Pt lines were made by focused ion beam milling; all other changes are by electron beam irradiation. Panels b−d and e−h show an unsuccessful and a successful run, respectively. Several insets in the figures b−h show schematic cross sections along the metal line direction. (b) With a short irradiation, a small hole in the Si_3N_4 membrane was made (see arrow). (c) Localized irradiations above and below the center of the bridge have reduced its width. An enlargement of the remaining bridge is given as inset. Fringes in the bridge are Pt(111) lattice planes with a spacing of 2.3 Å. (d) The beam was intentionally spread to capture the gap formation real time with a fast-scan CCD. This change in electron flux, however, resulted in a strong increase of the width of the bridge, after which no good control over the gap formation was possible. (e) An image taken about halfway the formation process of a second run. First a cut through the upper part of the bridge was made. During this process a relatively large grain was formed. Since the making of an electrode with this grain is not fully controllable, the shape of this large grain was changed, prior to manipulation of the rest of the bridge. The changed shape is given as inset in the upper left corner. (f,g,h) HREM images just before and after the formation of the gap in the lower part of the bridge. Exact measurement of the absolute value of the gap size is difficult due to the lens aberrations.

displacements are clearly visible in movies such as the one in ref 21. Diffusion along the beam direction also takes place, leading to the elongated grains that complicate the electrode formation. The easiest cuts through the polycrystalline lines were made when the size of the single crystalline grains was small (<5 nm), but resulted in the greatest changes in the electrode after its formation.

In general, TEM researchers have disfavored electron-beam-induced changes of materials, because these can generate artifacts in the starting materials. The formations of dislocations in metals and the amorphization of beam-sensitive materials are well known.[22] The former are the result of knock-out of atoms from their lattice position, while the latter is mainly due to ionization damage. On the other hand, electron-beam-induced deposition uses the decomposition of molecules on a surface by the focused electron beam, and electron-beam-induced changes of metals in the TEM can be used to study the structure of nanometer sized metal wires.[16−19] Our work shows that a TEM beam can be used favorably for the formation of nanoelectrodes to great precision. The determination of the gap with Å precision from the HREM images is difficult due to the aberrations of

the HREM. Thus, for this sculpturing, an aberration corrected HREM (that has recently become commercially available) is very useful as shown by Takai et al.[18]

A number of further improvements for the formation of nanoelectrodes in a TEM are conceivable. First, one can use single-crystalline instead of polycrystalline lines, e.g., via epitaxial growth on a single crystalline Si membrane and subsequent oxidation of the Si. This approach has the advantage that one can select a grain orientation for which the surface planes of the electrodes are relatively stable. Second, an increase of the specimen temperature during irradiation will likely accelerate sculpting of Pt. Third, further control of electron beam sculpting can be obtained by tuning the diameter, shape, and intensity of the electron beam in response to the observed changes of the material. Of course, the sculpting technique also allows for more complex structures than two electrodes with a narrow gap and it is well suited for combination with standard optical lithography and focused ion beam milling. An example is a gate near the gap, or, more complex but very exciting, a nanosensor consisting of a pore with electrodes nearby for rapid electrical detection of, e.g., single DNA strands in solid-state nanopores.[23]

To demonstrate the effectiveness of our technique for making nanoelectrodes, we trapped a small Au particle inside a TEM-fabricated electrode gap, measured its $I-V$ characteristics, and determined the geometry of the obtained nanodevice by TEM imaging. To trap a metal particle, we first covered the electrodes with a self-assembled monolayer of 1,4-benzenedithiol by immersing them in an ethanol solution for 2 h. No current could be measured across these electrodes for voltages up to 4 V. Subsequently, we put a small droplet of a 5 nm gold colloid solution (Sigma-Aldrich) diluted with ethanol on top of the electrodes and applied a voltage of 4 V for a few seconds using a series resistance of 1 GΩ. This trapping procedure is similar to the one used by Bezryadin et al.[24] Without delay, the electrodes were then extensively rinsed in ethanol and blown dry with dry nitrogen. One out of three devices remained nonconducting. TEM inspection of the non conducting ensemble showed that even though a gold particle was trapped between the electrodes, the width of one of the tunnel barriers was more than 1 nm. The other two devices had gold particles nicely situated between the electrodes with the resistances having changed from infinite to 20 and 500 MΩ, respectively.

The electrical measurements on the device depicted in Figure 3C show a Coulomb blockade suppression of the current even at room temperature. As can be seen from the low temperature measurement curve, the Coulomb gap is at least 220 mV, which corresponds to a total capacitance of the metal island of less than 2 aF. This is clearly compatible with the device geometry observed in Figure 3B. Assuming that the separation between the gold particle and the electrodes equals the length of one benzenedithiol molecule (∼0.6 nm), the capacitance of one tunnel junction can be calculated to be 0.9 aF. The total capacitance of the gold particle is thus approximately twice this value, in full agreement with the measurement. This suggests that it is possible to correlate the capacitance of ensembles with the size of the trapped particles and their position on the electrodes.

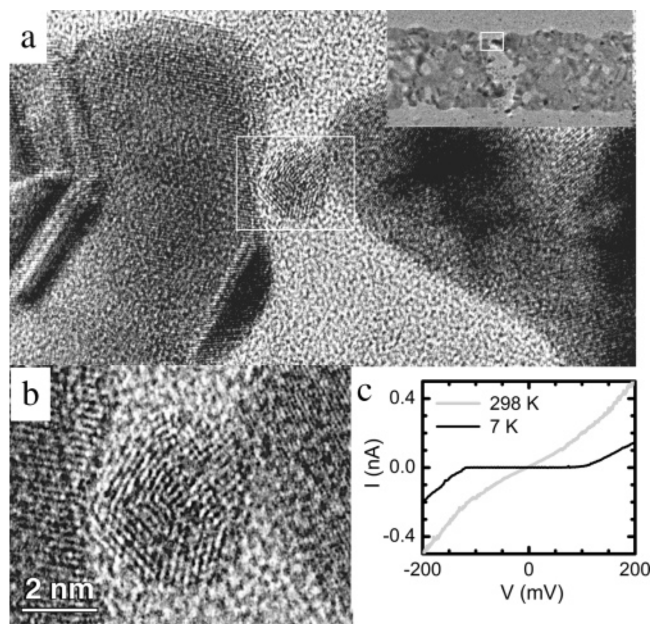

Figure 3. A gold particle trapped between two gold electrodes on a SiN membrane that had been sculpted with a transmission electron beam. The diameter of the gold particle is 4 nm. Lattice fringes with a spacing of 2.3 Å (left electrode) and 1.4 Å (right electrode) are distinguishable. (a) Overview of the electrodes (the line of which the electrodes are sculpted is given as inset in the upper right corner). (b) Au particle and its close surrounding. (c) Current−voltage measurements through the device at room temperature and at 7 K, respectively, clearly indicating Coulomb blockade.

The $I-V$ measurements shown in Figure 1C are in accordance with the single-electron tunneling behavior expected for such a device. While the current through small metal particles has been measured before,[24,25] the visual characterization of the ensemble shown in Figure 3A,B is of unprecedented clarity. This reveals the significance of being able to combine electrical measurements of nanostructures and their visual inspection with atomic precision.

In conclusion, we found that the electron beam of a normal transmission electron microscope is a very attractive tool for manufacturing electrodes with sub-nanometric precision, free-standing or on a supporting membrane. Nanoelectrodes made in polycrystalline Au showed continued slow relaxation after the electron beam irradiation. In contrast, nanoelectrodes made in polycrystalline Pt were stable and gap widths as low as 1 nanometer were obtained. Sculpting metals with a TEM is particularly suited for manufacturing single nanodevices quickly. We showed that nanoelectrodes made from gold in a TEM allow electrical and visual investigation of a trapped particle. This method can be used for single molecules, nanotubes, and other nanoparticles. More complex devices can be made as well, because the modifications induced by the electron beam can be visualized in real time during the most critical parts of the process.

Supporting Information Available: Movie showing the formation of a gap. This material is available free of charge via the Internet at http://pubs.acs.org.

References

(1) Tans, S. J.; Verschueren, A. R. M.; Dekker, C. *Nature* **1998**, *393*, 49.
(2) Park, H.; Park, J.; Lim, A. K. L.; Anderson, E. H.; Alivisatos, A. P.; McEuen, P. L. *Nature* **2000**, *407*, 57.
(3) Park, J.; Pasupathy, A. N.; Goldsmith, J. I.; Chang, C.; Yaish, Y.; Petta, J. R.; Rinkoski, M.; Sethna, J. P.; Abruna, H. D.; McEuen, P. L.; Ralph, D. C. *Nature* **2002**, *417*, 722.
(4) Aviram, A.; Ratner, M. A. *Chem. Phys. Lett.* **1974**, *29*, 277.
(5) Reed, M. A.; Zhou, C.; Muller, C. J.; Burgin, T. P.; Tour, J. M. *Science* **1997**, *278*, 252.
(6) Nygard, J.; Cobden, D. H.; Lindelof, P. E. *Nature* **2000**, *408*, 342.
(7) Kervennic, Y. V.; Van der Zant, H. S. J.; Morpurgo, A. F.; Gurevich, L.; Kouwenhoven, L. P. *Appl. Phys. Lett.* **2002**, *80*, 321.
(8) Kubatkin, S.; Danilov, A.; Hjort, M.; Cornil, J.; Brédas, J. L.; Stuhr-Hansen, N.; Hedegård, P.; Bjørnholm, T. *Nature* **2003**, *425*, 698.
(9) Guillorn, M. A.; Carr, D. W.; Tiberio, R. C.; Greenbaum, E.; Simpson, M. L. *J. Vac. Sci. Technol.* **2000**, B *18*, 1177.
(10) Carcenac, F.; Malaquin, L.; Vieu, C. *Microelectron. Eng.* **2002**, *61*, 657.
(11) Park, H.; Lim, A. K. L.; Alivisatos, A. P.; Park, J.; McEuen, P. L. *Appl. Phys. Lett.* **1999**, *75*, 301.
(12) Morpurgo, A. F.; Marcus, C. M.; Robinson, D. B. *Appl. Phys. Lett.* **1999**, *74*, 2084.
(13) He, H. X.; Boussaad, S.; Xu, B. Q.; Li, C. Z.; Tao, N. J. *J. Electroanal. Chem.* **2002**, *522*, 167.
(14) Storm, A. J.; Chen, J. H.; Ling, X. S.; Zandbergen, H. W.; Dekker, C. *Nat. Mater.* **2003**, *2*, 537.
(15) Troiani, H. E.; Miki-Yoshida, M.; Camacho-Bragado, G. A.; Marques, M. A. L.; Rubio, A.; Ascencio, J. A.; Jose-Yacaman, M. *Nano Lett.* **2003**, *3*, 751.
(16) Kondo, Y.; Takayanagi, K. *Phys. Rev. Lett.* **1997**, *79*, 3455.
(17) Rodrigues, V.; Fuhrer, T.; Ugarte, D. *Phys. Rev. Lett.* **2000**, *85*, 4124.
(18) Takai, Y.; Kawasaki, T.; Kimura Y.; Ikuta, T.; Shimizu, R. *Phys. Rev. Lett.* **2001**, *97*, 106105.
(19) Oshima, Y.; Kondo, Y.; Takayanagi, K. *J. Electron Microsc.* **2003**, *52*, 49.
(20) Kizuka, T. *Phys. Rev. Lett.* **1998**, *81*, 4448.
(21) The last 40 s of the movie can be downloaded from http://nchrem.tnw.tudelft.nl. See also Supporting Information.
(22) Williams D. C.; Carter C. B. *Transmission electron microscopy; a textbook for materials science*; Plenum Press: New York, 1996.
(23) Howorka, S.; Cheley, S.; Bayley, H. *Nat. Biotech.* **2001**, *19*, 636.
(24) Bezryadin, A.; Dekker, C. Schmid, G. *Appl. Phys. Lett.* **1997**, *71*, 1273.
(25) Tinkham M.; Davidovic D.; Ralph D. C.; Black C. T. *J. Low Temp. Phys.* **2000**, *118*, 271.

NL050106Y